Synthesis of Sn-Porphyrin-Intercalated Trititanate Nanofibers: Optoelectronic Properties and Photocatalytic Activities

Joon Hee Jang,[†] Ki-Seok Jeon,[†] Seungdo Oh,[†] Hee-Joon Kim,[§] Tsuyoshi Asahi,[‡] Hiroshi Masuhara,[‡] and Minjoong Yoon*[,†]

Department of Chemistry, Chungnam National University, Daejeon, 305-764, Korea, Department of Applied Physics, Osaka University, Osaka, Japan, and Department of Applied Chemistry, Kumoh National Institute of Technology, Gumi, Korea

Received December 16, 2006. Revised Manuscript Received January 30, 2007

A new class of nanostructures were fabricated by one-step hydrothermal reaction of a mixture solution of TiO_2 anatase powder and a Sn-porphyrin, *trans*-dihydroxo[5,10,15,20-tetrakis(*p*-tolyl)porphyrinato]-tin(IV) [SnTTP], and they were found to be well-crystalline trititanate ($H_2Ti_3O_7$)-type multilayered nanofibers (TiNFs) intercalated by SnTTP which have lengths in the range of 0.5−1 μm with an average diameter of approximately 50 nm. Based on the femtosecond-diffuse reflectance transient absorption and photoluminescence spectroscopic measurements, the SnTTP-intercalated TiNFs were observed to exhibit efficient optoelectronic properties such as photoinduced electron transfer from deep surface states of trititanate layer to SnTTP, forming an anion radical $SnTTP^{\bullet -}$ rapidly in a few picoseconds. These results infer that electrons and holes are effectively separated in the SnTTP−TiNFs upon illumination, and consequently remarkable UV−visible light-sensitive photocatalytic activities as compared to those of free TiNFs and SnTTP, suggesting that the SnTTP-intercalated TiNFs have potential application in development of efficient artificial photosynthetic systems and photoelectronic materials.

Introduction

TiO_2 nanomaterials are of great current interest for applications in photoelectronics, light-energy conversion, artificial photosynthetic systems, and photocatalysis.[1−3] The success of these applications relies on the recombination dynamics of the electron and hole (excitons) on the surface of the TiO_2 nanomaterials, and it is important to control the recombination dynamics of the surface excitons. Thus, in the past decades, the use of low-dimensional TiO_2 nanostructures such as nanotubes and nanofibers have attracted considerable attention from the materials science community as one of the most promising options to control the exciton dynamics to improve the photoactivity[4,5] because the intercrystalline contacts of TiO_2 can be highly decreased to facilitate electron transfer through the titania layer with high BET specific surface area.

The TiO_2 nanotubes of the anatase phase have been synthesized by porous alumina templating, sol−gel, and hydrolytic routes which require multistep processes.[4,6,7] An interesting synthesis alternative was to obtain needle-shaped nanotubes, nanofibers, and nanowires by one-step hydrothermal treatment of TiO_2 powders in 5−15 M NaOH solution at different digestion temperatures.[8−12] However, these nanostructures are not either anatase or rutile but trititanate ($H_2Ti_3O_7$) phase,[13−15] and do not inherit the efficient photocatalytic activity as compared to the anatase nanostructures. Nevertheless, we have recently found, by the picosecond time-resolved photoluminescence studies, that the separation of photoinduced electron−hole in the trititanate nanostructures is more efficient than that in anatase titania quantum dots.[16] Therefore, if the trititanate building blocks are modified by incorporation with a good electron-relay metal, semiconductor, or molecule, a new class of photofunctional trititanate nanostructures would be obtained. Interestingly, one-dimensional Fe chain-intercalated trititanate nanotubes were synthesized and observed to release differences in electronic and optical properties as compared to those of the naked nanotubes,[17] but no photocatalytic

* Corresponding author. E-mail: mjyoon@cnu.ac.kr. Fax: 82-42-823-7008.
[†] Chungnam National University.
[‡] Osaka University.
[§] Kumoh National Institute of Technology.

(1) Fujishima, A.; Hashimoto, K.; Watanabe, T. In *TiO_2 Photocatalysis: Fundamentals and Applcation*; BKC, Inc.: Tokyo, Japan, 1999.
(2) Hagfeldtt, A.; Grätzel, M. *Chem. Rev.* **1995**, *95*, 49−68.
(3) Yoon, M.; Chang, J. A.; Kim, Y.; Choi, J. R.; Kim, K.; Lee, S. J. *J. Phys. Chem. B* **2001**, *105*, 2539−2545.
(4) Adachi, M.; Murata, Y.; Okada, I.; Yoshikawa, S. *J. Electrochem. Soc.* **2003**, *150*, G488−G493.
(5) Zhao, J.; Wang, X.; Chen, R.; Li, L. *Solid State Commun.* **2005**, *134*, 705−710.
(6) Hoyer, P. *Langmuir* **1996**, *12*, 1411−1413.
(7) Mao, Y.; Wong, S. S. *J. Am. Chem. Soc.* **2006**, *128*, 8226−8228.
(8) Kasuga, T.; Hiramatsu, M.; Hoson, A.; Sekino, T.; Niihara, K. *Adv. Mater.* **1999**, *11*, 1307−1310.
(9) Seo, D.-S.; Lee, J.-K.; Kim, H. *J. Cryst. Growth* **2001**, *229*, 428−432.
(10) Yuan, Z.-Y.; Su, B.-L. *Colloid Surf., A* **2004**, *241*, 173−183.
(11) Wu, D.; Liu, J.; Zhao, X.; Li, A.; Chen, Y.; Ming, N. *Chem. Mater.* **2006**, *18*, 547−553.
(12) Zhu, H.; Gao, X.; Lan, Y.; Song, D.; Xi, Y.; Zhao, J. *J. Am. Chem. Soc.* **2004**, *126*, 8380−8381.
(13) Chen, Q.; Du, G. H.; Zhang, S.; Peng, L.-M. *Acta. Crystallogr.* **2002**, *B58*, 587−593.
(14) Zhang, S.; Peng, L.-M.; Chen, Q.; Du, G. H.; Dawson, G.; Zhou, W. Z. *Phys. Rev. Lett.* **2003**, *91*, 256103−256104.
(15) Suzukia, Y.; Yoshikawa, S. *J. Mater. Res.* **2004**, *19*, 982−985.
(16) Jang, J. H.; Jeon, K.-S.; Park, T.-S.; Lee, K. W.; Yoon, M. *J. Chin. Chem. Soc.* **2006**, *53*, 123−130.

10.1021/cm0629863 CCC: $37.00
Published on Web 03/23/2007

activities were effective. On the other hand, Hodos et al. prepared the CdS-doped trititanate nanotubes and observed their photocatalytic activity for the reduction of methyl orange.[18] Zhu et al.[12] also prepared the trititanate nanofibers covered with anatase nanocrystal and observed enhancement of the photocatalytic activity for decomposition of sulforhodamine. However, CdS or anatase TiO_2 nanocrystal itself has high photocatalytic activity under the light illumination,[19,20] and it is not so clear whether the photocatalytic activity of the modified trititanate nanostructures is improved by assistance of the doped CdS or surface-covered anatase TiO_2. Moreover, there is no direct evidence provided for the photoinduced electron or hole transfer for the phocatalytic activity in the modified trititanate nanofibers. Thus, there is a need for well-defined trititanate nanostructures modified by using an electron relay molecule.

Herein, to design not only the highly efficient nanostructural photocatalysts but also photoelectronic materials, we synthesized new photoactive trititanate ($H_2Ti_3O_7$)-type TiO_2 nanofibers by intercalating the electron acceptor molecule such as a *trans*-dihydroxo[5,10,15,20-tetrakis(*p*-tolyl)porphyrinato]tin(IV) [SnTTP][21] into the trititanate layers through one-step hydrothermal reaction[22,23] and analyzed their crystal phase and morphologies using FT-IR, XRD, TEM, and AFM. Thereafter, we examined the optoelectronic properties such as photoinduced electron transfer and its dynamics in the porphyrin−trititanate nanocomposites by using femtosecond (fs)-transient diffuse reflectance absorption and photoluminescence spectral techniques, confirming that the porphyrin−trititanate hybrid composites have highly photocatalytic activities.

By the way, the synthetic porphyrins are often self-organized and they have been used as attractive building blocks for photoelectronic functional supramolecular systems[24,25] or nanostructures,[26−28] and particularly the metalloporphyrins including tin-porphyrins have been of great interest as analogues of chlorophyll to develop artificial photosynthetic systems splitting water to evolve hydrogen in the presence of catalysts.[29,30] Also well-defined *J*-aggregate-type tin-porphyrin nanotubes[31] mimicking the light-harvesting rods of the aggregated green-sulfur bacteriochlorophyl[32−34] were synthesized by ionic self-assembly of two oppositely charged porphyrins. However, their naked morphologies are not so stable in the light,[31] and they have some limitations in applications in the artificial photosynthetic systems. In this point of view, the intercalation of porphyrins into the trititanate nanostructures would be a good model for protection of the porphyrin aggregates from light damage.

Experimental Section

Materials. The chemicals for the synthesis of the new trititanate nanostructures, titanium(IV) isopropoxide (Aldrich), anantase TiO_2 powder, and ethanol (>99.9%, Merck), were used as received. *trans*-Dihydroxo [5,10,15,20-tetrakis(*p*-tolyl)porphyrynato]tin(IV) (SnTTP) was prepared by the modified literature method[22] by using *trans*-dichloro-[5,10,15,20-tetrakis (*p*-tolyl)porphyrinato]tin(IV) ($SnCl_2$-TTP) which was prepared according to the reported procedures.[35] A mixture of $SnCl_2$TTP (0.450 g, 0.524 mmol) and potassium carbonate (1.14 g, 8.89 mmol) in tetrahydrofuran (400 mL) and water (100 mL) was heated at reflux for 4 h. The organic solvent was removed and the aqueous layer was extracted into CH_2Cl_2. The organic layer was washed with water, then dried over anhydrous $MgSO_4$, and filtered and then the solvent was removed to give the crude product, followed by recrystallization from CH_2Cl_2/hexane to give (TTP)Sn(OH)$_2$. Yield: 0.365 g (85%). ^{1}H NMR (500 MHz, $CDCl_3$): 9.13 (s, 8H, -pyrrolic H), 8.21 (d, 8H, *o*-Ph), 7.62 (d, 8H, *m*-Ph), 2.73 (s, 12H, CH_3), −7.49 (s, 2H, OH).

Synthesis of Sn-Porphyrin-Intercalated Trititanate Nanofibers. To fabricate the Sn-porphyrin-intercalated trititanate nanofibers, 10 mL of ethanol solution of *trans*-dihydroxo [5,10,15,20-tetrakis (*p*-tolyl)porphyrinato]tin(IV) (SnTTP) (5×10^{-5} M) was mixed with 10 mL of 5 M NaOH aqueous solution. Fifty milligrams of TiO_2 anatase powder (Yakuri Pure Chemicals, extra pure grade) was added into the mixed solution of SnTTP, followed by hydrothermal digestion in a sealed Teflon autoclave by statically heating at 200 °C for 24 h. After the hydrothermal reaction, the solution containing precipitates was diluted in 500 mL of deionized water to prevent the membrane filter paper from damage due to low pH condition. The precipitates were filtered using membrane filter (Millipore, 0.1 μm VCTP membrane filter) and washed with 3 L of deionized water and 500 mL of ethanol to remove physically absorbed SnTTP on the surface of precipitates. The final products were obtained after drying at 50 °C. The relative amount of intercalated SnTTP in the produced materials was determined by thermo-gravimetric-differential thermal analysis (TG-DTA) using TA instruments SDT 2960 simultaneous DTA-TGA.

(17) Xu, X. G.; Ding, X.; Chen, Q.; Peng, L.-M. *Phys. Rev. B* **2006**, *73*, 165403.
(18) Hodos, M.; Horváth, E.; Haspel, H.; Kukovecz, Á.; Kónya, Z.; Kiricsi, I. *Chem. Phys. Lett.* **2004**, *399*, 512−515.
(19) Karunakaran, C.; Senthilvelan, S. *Sol. Energy* **2005**, *79*, 505−512.
(20) Yang, H.; Huang, C.; Li, X.; Shi, R.; Zhang, K. *Mater. Chem. Phys.* **2005**, *90*, 155−158.
(21) O'Rourke, M.; Curran, C. *J. Am. Chem. Soc.* **1970**, *92*, 1501−1505.
(22) Arnold, D. P. *J. Chem. Educ.* **1988**, *65*, 1111−1112.
(23) Yoshikawa, H.; Kurokawa, N.; Yokote, Y.; Namba, S.; Masuhara, H. *Handai Nano-photonics*; Masuhara, H., Kawata, S., Eds.; Elsevier, Netherlands, 2004; Vol. 1, Chapter 15.
(24) (a) Osuka, A.; Shimidzu, H. *Angw. Chem., Int. Ed. Engl.* **1997**, *36*, 135. (b) Aratani, N.; Osuka, A.; Kim, D.; Kim, Y. H.; Jeong, D. H. *Angew. Chem., Int. Ed.* **2000**, *39*, 1458. (c) Kim, D.; Osuka, A. *J. Phys. Chem. A* **2003**, *107*, 8791−8816. (d) Nakamura, Y.; Hwang, I.-W.; Aratani, N.; Ahn, T. K.; Ko, D. M.; Takagi, A.; Kawai, T.; Matsumoto, T.; Kim, D.; Osuka, A. *J. Am. Chem. Soc.* **2005**, *127*, 236−246. (e) Ahn, T. K.; Kim, K. S.; Kim, D. Y.; Noh, S. B.; Aratani, N.; Ikeda, C.; Osuka, A.; Kim, D. *J. Am. Chem. Soc.* **2006**, *128*, 1700−1704.
(25) (a) Daphnomili, D.; Scheidt, W. R.; Zajicek, J.; Coutsolelos, A. G. *Inorg. Chem.* **1998**, *37*, 3675−3681. (b) Raptopoulou, C.; Daphnomili, D.; Karamalides, A.; Di Vaira, M.; Terzis' A.; Coutsolelos, A. G. *Polyhedron* **2004**, *23*, 1777−1784.
(26) Furshop, J.-H.; Binding, U.; Siggel, U. *J. Am. Chem. Soc.* **1993**, *115*, 11036−11037.
(27) Schwab, A. D.; Smith, D. E.; Rich, C. S.; Young, E. R.; Smith, W. F.; de Pola, J. C. *J. Phys. Chem. B* **2003**, *107*, 11339−11345.
(28) Rotomkis, R.; Augulis, R.; Snitka, V.; Valiokas, R.; Liedberg, B. *J. Phys. Chem. B* **2004**, *108*, 1833−1838.
(29) Hosono, H. *Chem. Lett.* **1997**, 523−524.
(30) Wang, S.; Tabata, I.; Hisada, K.; Hori, T. *Dyes Pigm.* **2002**, *55*, 27−33.
(31) (a) Wang, Z.; Medforth, C. J.; Shelnutt, J. A. *J. Am. Chem. Soc.* **2004**, *126*, 15954−15955. (b) Wang, Z.; Medforth, C. J.; Shelnutt, J. A. *J. Am. Chem. Soc.* **2004**, *126*, 16720−16721.
(32) van Rossum, B.-J.; Steensgaard, D. B.; Mulder, F. M.; Boender, G. J.; Schaffner, K.; Holzwarth, A. R.; de Groot, H. J. M. *Biochemistry* **2001**, *40*, 1587−1595.
(33) Blankenship, R. E.; Olson, J. M.; Miller, M. *Antenna Complexes from Green Photosythetic Bacteria;* Kluwer Academic Publishers: Dordrecht, The Netherlands, 1995.
(34) Olsonl, J. M. *Photochem. Photobiol.* **1998**, *67*, 61−75.
(35) Crossley, M. J.; Thordarson, P.; Wu, R. A.-S. *J. Chem. Soc., Perkin Trans. 1* **2001**, 2294−2302.

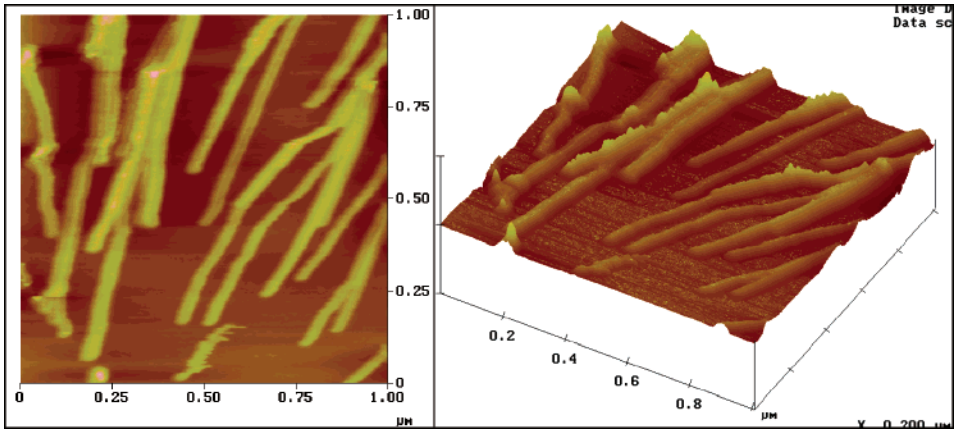

Figure 1. Tapping mode AFM images of the as-synthesized SnTTP-intercalated TiO_2 nanostructures dispersed on highly oriented pyrolytic graphite (HOPG).

For comparison purposes, free trititanate nanofibers (TiNFs) were also prepared under the same conditions as those for the preparation of SnTTP-intercalated TiNFs except addition of SnTTP.

Structural Characterization of Nanofibers. The crystalline phase of the produced materials was characterized by recording X-ray diffraction (XRD) patterns on a Rigaku Rotaflex diffractometer (Model No. D/MAX-2200 Ultima/PC, rotating Cu Kα target, 3 kW X-ray and set to 40 kV and 40 mA) at an X-ray incident angle of 0.02°. The morphology of the synthesized materials was examined by transmission electron microscope (TEM) (JEOL JEM-2010, Japan) and atomic force microscope (AFM) (NanoScopeIIIA, DI, USA). Samples for TEM measurement were prepared by dip coating Formvar/carbon film Cu grids with nanocolloidal solution obtained by sonicating the produced powder material in ethanol. On the other hand, AFM images were measured by tapping mode by using samples prepared by dip coating the dispersed solution on highly oriented pyrolytic graphite (HOPG).

Steady-State Spectroscopic Measurements. Diffuse reflectance UV−visible absorption spectra and FT-IR spectra were also measured to recognize the interposition of the produced materials. Diffuse reflectance UV−visible absorption spectra were recorded on a Shimadzu UV-3101PC spectrophotometer and Varian Cary 3E UV−visible spectrophotometer for powder sample and ethanol solution, respectively. FT-IR spectra were obtained by using a JASCO FT/IR-4100 spectrophotometer at a resolution of 2 cm^{-1} and compared with that of SnTTP.

Photoluminescence (PL) spectra were measured on a scanning SLM-AMINCO 4800 spectrofluorometer with the synthesized nanofiber powders dispersed in water (0.03 g/L). Before the PL measurement, the sample solution was bubbled with high-purity Ar to remove the dissolved oxygen. The single nanoparticle photoluminescence spectra were also measured to avoid the inhomogeneous size distribution effects of the photophysical properties of the nanofibers (see Supporting Information).

fs-Diffuse Reflectance Transient Absorption Spectral Measurements. The details of the fs-diffuse reflectance spectroscopic system have been reported elsewhere.[36,37] Briefly, a light source consists of a cw self-mode-locked Ti:sapphire laser (Mira 900) Basic, Coherent) pumped by an Ar^+ laser (Innova 310, Coherent) and a Ti:sapphire regenerative amplifier system (TR 70, Continuum) with a Q-switched Nd:YAG laser (Surelight I Continuum). The fundamental output from the regenerative amplifier (780 nm, 3−4 mJ/pulse, 170 fs fwhm, 10 Hz) was frequency-doubled (390 nm) and used as an excitation light pulse. The energy of the excitation pulse measured with a Joule meter (P25, Scientech) was several tens of microjoules and its spot size on the sample was nearly 2 mm. The shot-to-shot fluctuation of the energy was less than ±10%. The residual of the fundamental output was focused into a quartz cell (1 cm path length) containing H_2O to generate a white-light continuum as a probe pulse. Transient absorption intensity was displayed as percentage absorption,[37]

$$\% \text{ absorption} = 100 \times (1 - R/R_0)$$

where R and R_0 represent intensity of the diffuse reflected light of the probe pulse with and without excitation, respectively. The time resolution of the system is shorter than 1 ps for the powder having a large absorption coefficient.

Measurement of Photocatalytic Activities. Photocatalytic activities were assessed by monitoring photo-oxidation of methyl orange (MO) in aqueous solution containing the SnTTP-intercalated trititanate nanofibers or free trititanate nanofibers as photocatalysts as previously reported.[38] Five milligrams of the nanofibers was mixed with 10 mL of the aqueous MO solution (5×10^{-6} M) in optically matched Pyrex test tubes, and the mixed solutions were simultaneously irradiated under oxygen flow. The visible light irradiation was carried out with 450 W Hg lamp using cutoff filters (400 nm). The UV-light irradiation was carried out with 355 nm Nd:YAG laser. After a certain period of irradiation, each solution was centrifuged to sediment the photocatalysts, followed by taking the supernatant solution to measure the absorption spectral change of MO at 474 nm to monitor the photooxidation. The photocatalytic quantum efficiency was determined by ferrioxalate actinometric method[39] via measurement of the power of the irradiation light from the Hg lamp and Nd:YAG laser.

Results and Discussion

Structural Characterization. Figure 1 shows atomic AFM images of the as-synthesized powders coated on a HOPG, showing that the hydrothermal reaction seems to provide a high yield of two-dimensional nanostructures with little dispersion in diameters. Most of the nanostructures (95%) were 600 nm in length and have diameters in the range of 30−50 nm, and the remaining 5% was observed to have exceptionally large dimensions (∼300 nm in diameter and micrometers in length). It is interesting to note that the sizes of the nanostructures are larger than those of free TiO_2

(36) Asahi, T.; Furube, A.; Fukumura, H.; Ichikawa, M.; Masuhara, H. *Rev. Sci. Instrum.* **1998**, *69*, 361−371.
(37) Furube, A.; Asahi, T.; Masuhara, H.; Yamashita, H.; Anpo, M. *J. Phys. Chem. B* **1999**, *103*, 3120−3127.
(38) Yoon, M.; Seo, M.; Jeong, C.; Jang, J. H.; Jeon, K. S. *Chem. Mater.* **2005**, *17*, 6069−6079.
(39) Suppan, P. *Chemistry and Light*; Royal Society of Chemistry: Cambridge, U.K., 1994; Chapter 7, pp 254−255.

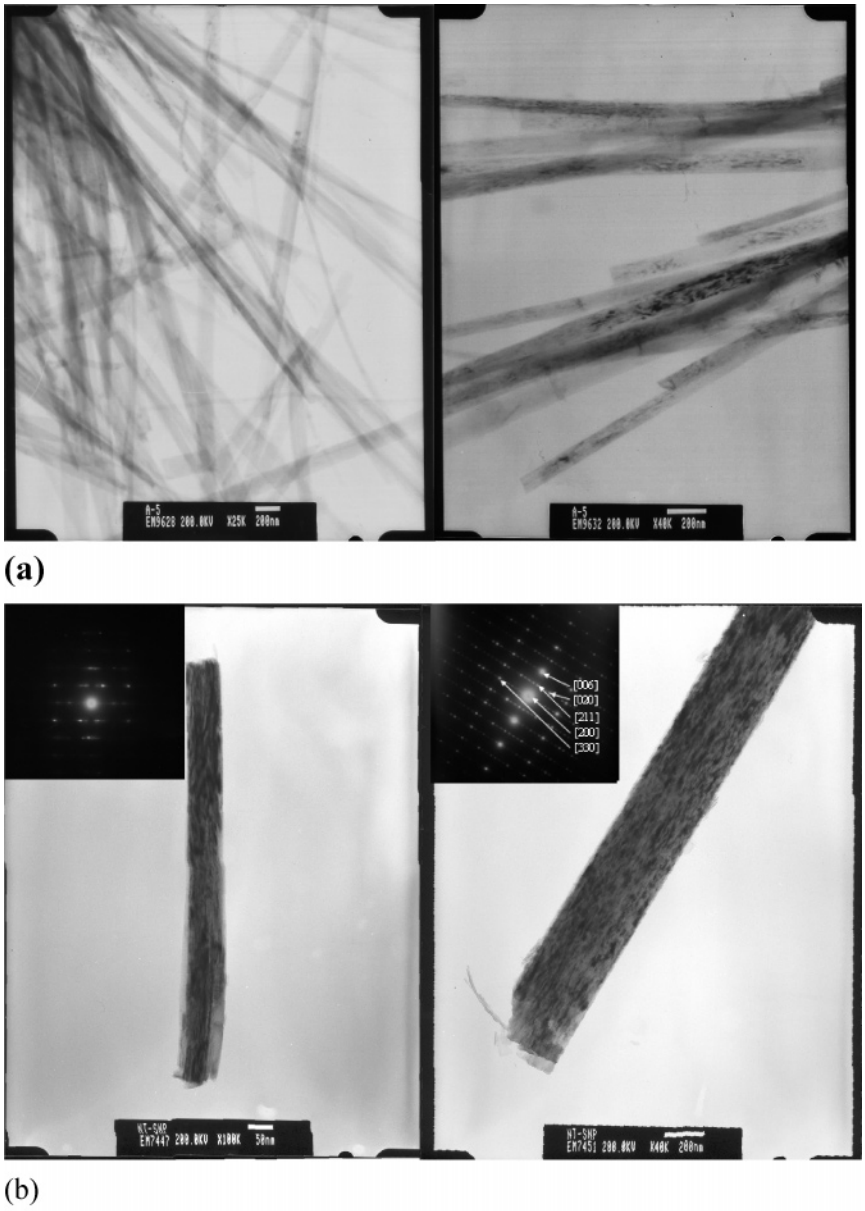

Figure 2. (a) Low-magnification TEM images of SnTTP−TiNFs. (b) High-resolution TEM images of the two selected single SnTTP−TiNTs of different dimensions.

nanostructures such as nanotubes or nanofibers (∼10 nm).[14] The synthesized nanostructures were also identified from TEM measurements (Figures 2a and 2b). However, it is noteworthy that no hollows were observed from the newly synthesized nanostructures, indicating that the synthesized nanostructures have a fibroid nature rather than tubes. The formation of the nanofibers may be due to the hydrothermal digestion at 200 °C as previously reported by many other groups.[40] Figure 2b shows TEM images of two selected single nanofibers of different sizes (50 and 300 nm in diameters) which have dark stripes. The dark stripes are not observable from free TiO_2 nanofibers (s-Figure 1), and they must have originated from aggregated SnTTPs intercalated into TiO_2 nanofibers (TiNFs), as confirmed by the UV−visible diffuse reflectance absorption spectrum of the synthesized nanofibers (Figure 3), which exhibit the combinatorial spectral features of both titania and porphyrins in the wavelength range from 250 to 700 nm. The relative amount

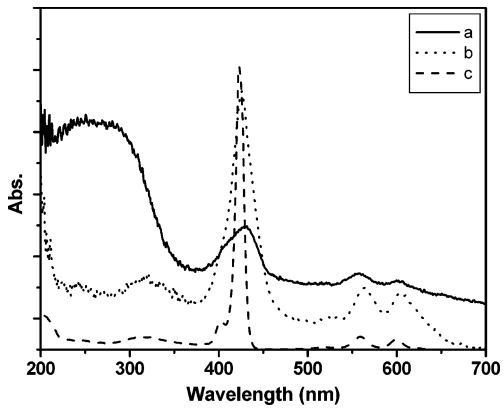

Figure 3. Diffuse reflectance UV−visible absorption spectra of SnTTP−TiNFs (a) and SnTTP powders (b). The absorption spectrum of diluted aqueous solution of SnTTP (5.0×10^{-6} M) corresponding to that of SnTTP monomer (c).

(40) Zhu, H. Y.; Lan, Y.; Gao, X. P.; Ringer, Zheng, Z. F.; Song, D. Y.; Zhao, J. C. *J. Am. Chem. Soc.* **2005**, *127*, 6730−6736.

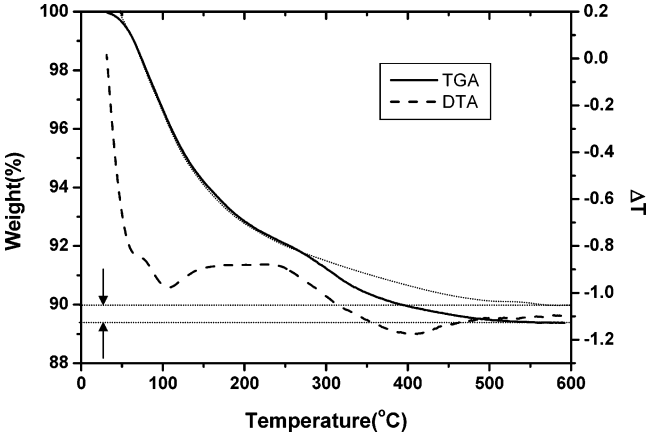

Figure 4. TG-DTA diagram of SnTTP−TiNFs. The TGA curve and DTA curves are represented by a solid line and a dotted line, respectively. The TGA curve is extrapolated to 600 °C, assuming that no SnTTP is involved in the weight decrease.

of intercalated SnTTP in the SnTTP-intercalated TiNFs (SnTTP−TiNFs) was determined by thermogravimetric-differential thermal analysis (TG-DTA) (Figure 4). The TGA curve shows a decrease of initial sample weight (4.769 mg) in two steps with the temperature increased, exhibiting an inflection point at 290 °C. According to the DTA, the decrease of the sample weight was analyzed to show two minimum differential points at 100 °C and second 400 °C. This indicates that the vaporization of water takes place first from the surface of the nanofibers followed by vaporization of the intercalated SnTTP as observed by the color change from yellow to white. If there is no SnTTP, the TGA curve should continuously decrease without the inflection point. The second decrease of the sample weight from 290 °C corresponds to the weight of the intercalated SnTTP as shown in the figure, and the estimated SnTTP is 0.56% of initial sample weight.

The selected area electron diffraction (SAED) patterns of both nanofibers (inset of Figure 2b) have also been observed to exhibit numerous ordered diffraction spots characteristic of typical trititanate crystal,[10,14,15] indicating that the SnTTP-intercalated TiNFs (SnTTP−TiNFs) are very well crystallized trititanate-type nanofibers. The trititanate-type crystallinity of the synthesized nanofibers is also supported by observation of their sharply resolved XRD peaks corresponding to the [200], [110], [221], [31$\bar{2}$], [113], [020], and [422] crystal faces of trititanate nanocystals.[10,14,15] The sharp XRD peaks must be attributed to the increased crystal size as compared to those of free trititanate nanofibers having the diameter of 9 nm with length of several hundreds of nanometers as shown in Figure 5b. Interestingly, the electron diffraction spots in the SAED pattern are seen to be elongated along the direction perpendicular to the fiber axis, being indexed to be [200], [211], [020], [006], and [330] planes, confirming that SnTTP−TiNFs are a class of multilayered spiral trititanate nanofibers which are constructed by wrapping a [200] sheet of trititanate along [001] as in the case of the formation of trititanate nanotubes.[13,14]

It is also noteworthy that the XRD peak of the (200) plane of SnTTP−TiNF showed slight decrement of the 2θ value to 10.6° from that of free tritianate nanofibers (11.2°) (Figure 5), indicating that the intershell *d*-spacing between the

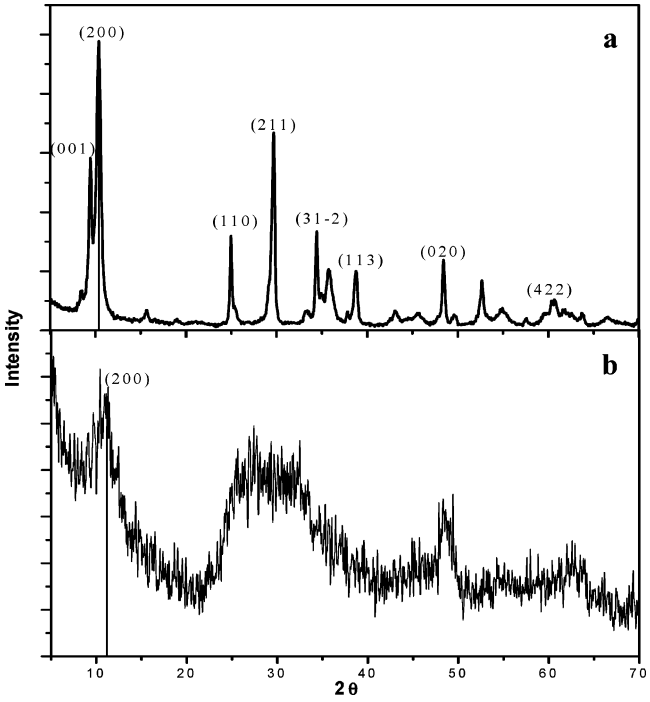

Figure 5. X-ray diffraction patterns of SnTTP−TiNFs (a) and free trititanate nanofibers (b).

trititanate layers of SnTTP−TiNT increased from 7.8 to 8.3 Å. The increase of *d*-spacing may be due to interposition of SnTPP between the layers consisting of [200] trititanate sheets as shown in the structure model (Figure 6) as proposed on the basis of the reported formation mechanism of the free trititanate nanotubes.[10,14] As Zhang et al. reported,[14] hydrothermal reaction of crystalline TiO_2 with NaOH results in growth of some trititanate-type plates through formation of a disordered phase, from which H-deficient individual thin Ti_3O_7 layers are peeled off. Consequently, SnTTP may be chemisorbed on the surface of Ti_3O_7 layer through Sn−O−Ti[41] since SnTTP has two axial OH ligands and is oxophilic. The chemisorption results in formation of an asymmetric environment of the Ti_3O_7 layer so that the layer scrolls to form the multilayered nanofibers intercalated with SnTTP. Interestingly, Yang et al.[20] also reported that a one-dimensinal chain of Fe atoms is intercalated between Ti_3O_7 layers of the trititanate nanotubes. Thus, it can be speculated that scrolling of Ti_3O_7 layer adsorbed with SnTPPs results in interposition of SnTTPs between Ti_3O_7 layers, forming the linkages of Ti−O−Sn−O−Ti, as supported by the FT-IR spectrum of SnTPP−TiNFs (Figure 7), showing broadening of O−H and Ti−O stretching bands around 3000 and 500−900 cm^{-1}, respectively, as compared to those of free trititanate nanofibers. Based on the known bond lengths of Sn−O and Ti−O (2.09 and 2.01 Å, respectively),[42,43] the bond length of the Ti−O−Sn−O−Ti was determined to be 8.20 Å which is about the same as the intershell *d*-spacing between the (200) layers as determined from the XRD data. It is known that the number of layers of free trititanate cannot

(41) Andou, Y.; Shiragami, T.; Shima, K.; Yasuda, M. *J, Photochem. Photobiol. A: Chem.* **2002**, *147*, 191−197.
(42) Shannon, R. D.; Prewitt, C. T. *Acta Crystallogr.* **1969**, *B25*, 925−946.
(43) Shannon, R. D.; Prewitt, C. T. *Acta Crystallogr.* **1970**, *B26*, 1046−1048.

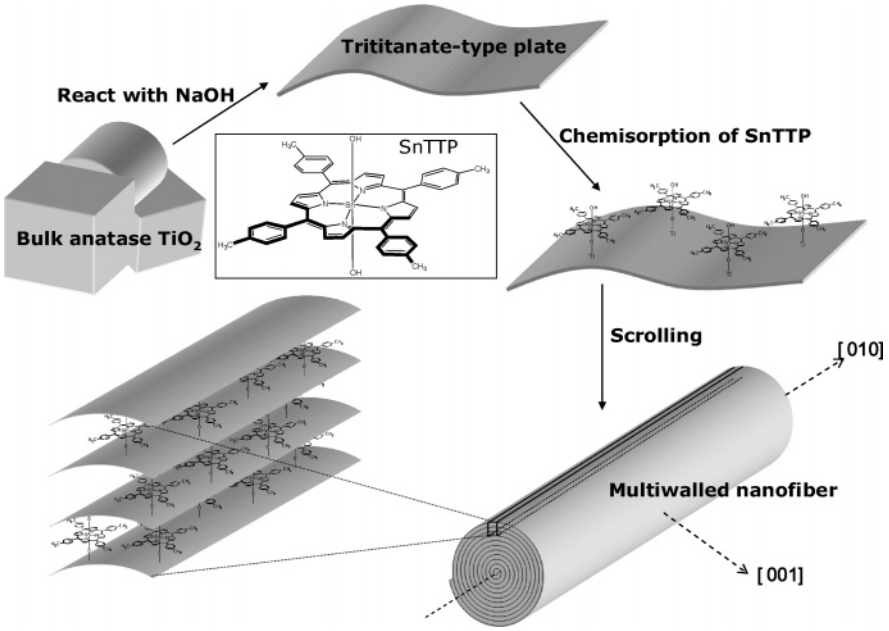

Figure 6. Schematic structure model of SnTTP−TiNF formed by rolling the SnTTP-adsorbed trititanate sheet along the [010] direction with a chiral vector along the [001] direction.

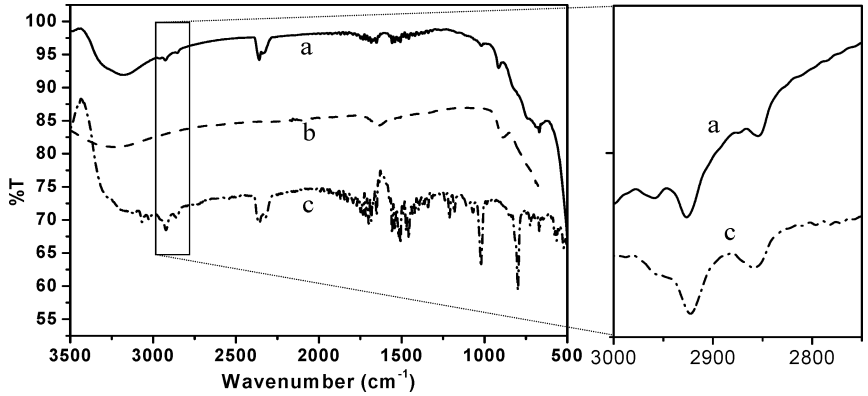

Figure 7. FT-IR spectra of SnTTP−TiNFs (a), free trititanate nanofibers (b), and SnTTP (c).

be increased from 4 due to repulsive force between upper and lower layers.[11] However, the repulsive force of the layers may be reduced by the intercalated SnTTP, and more scrolled layers will be available. This may be the reason why the SnTTP−TiNFs are formed with diameters much larger than those of free trititanate nanofibers.

Optoelectronic Properties. The SnTTP−TiNFs were observed to exhibit some interesting and potentially useful optoelectronic properties. The porphyrins intercalated into the layers of the nanofibers are supposed to be aggregated as their UV−visible absorption spectral bands are broadened as compared to the monomer bands and even broader than those of the condensed solid state of SnTTP (Figure 3). However, no significant red shifts were observed, indicating existence of non-J-aggregates of SnTTP in the trititanate nanofibers, The reason for the band broadening of the nanofibers is not unambiguously understood at the moment, but it might be suggested to be due to one possibility that the coherent coupling of the transition dipoles may span porphyrin molecules through coplanar interaction in parallel with trititanate layers as shown in Figure 6. If that is the case, such aggregate type may be beneficial to induce a cascade of the photoinduced electrons from the parallel trititanate layers, probably causing an efficient polarized electron transfer without photodamaging of the porphyrin aggregates.

To examine the possibility of the photoinduced electron transfer in the nanofibers, the photoluminescence (PL) emission spectra of the aqueous dispersion of SnTTP−TiNFs and free trititanate nanofibers were measured as shown in Figure 8. The free trititanate nanofibers exhibit broad surface emission in the range from 450 to 600 nm as well as the emission at 650 nm with excitation at 360 (Figure 8a), which are originated from the deep exciton trapped surface states and the defect levels such as oxygen vacancies, respectively.[16] When the SnTTP−TiNFs are excited at 420 nm, which is absorbed by SnTTP only, the typical SnTTP emission bands were observed at 610 and 665 nm without the deep surface emission bands (Figure 8b). However, when the SnTTP−TiNFs are excited at 360 nm, which are absorbed mostly by trititanate, both the deep surface emission of trititanate and the SnTTP emission were observed to be entirely quenched while the defect level emission at 650 nm of trititanate is unquenched (Figure 8c). Similarly, the single nanoparticle PL spectrum of SnTTP−TiNFs was also observed to exhibit the 650 nm emission only with excitation

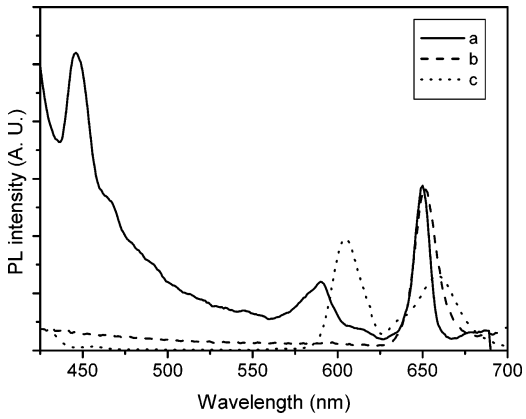

Figure 8. Photoluminescence emission spectra of free trititanate nanofibers (λ_{ex} = 360 nm) (a) and SnTTP−TiNFs (λ_{ex} = 360 nm (b), λ_{ex} = 420 nm (c)).

at 405 nm whereas that of free trititanate exhibits all the surface emission bands (s-Figure 2, Supporting Information). These results indicate that the photoinduced electrons trapped in the deep surface states are efficiently transferred to the intercalated SnTTP, forming an anion radical $SnTTP^{\bullet -}$ which is known to be nonfluorescent,[29] suggesting that recombination of electron and hole pairs produced from trititanate is inhibited by SnTTP.

To further explore the photoinduced electron transfer and its dynamics, the fs-time-resolved diffuse reflectance transient absorption spectra of both free trititanate nanofibers and SnTTP−TiNTs were measured. Figure 9 shows development and decay of the transient absorption spectra of free trititanante nanofibers (a) and SnTTP−TiNFs (b) as a function of delay time upon excitation at 390 nm. The nanofibers exhibit two broad transient absorption spectra centered at 500 nm immediately after excitation and at 700 nm over 10 ps (Figure 9a), which are attributed to electrons trapped in different surface states as commonly observed from Q-sized TiO_2 powders.[44] The trapped electrons exhibited two decay components (2 ps and >10 ns), indicating that at least two kinds of electrons, whose disappearance pathways are different from each other, are generated.[16] The shorter decay time component may be ascribed to the disappearance of electrons through interaction with phonons, while the longer component is attributed to recombination of deep surface state-trapped electrons with holes. On the other hand, the development features of the transient absorption bands for SnTTP−TiNFs (Figure 9b) are different from those observed for the free trititanate nanofibers. The spectra exhibited new transient bands around 560, 620, and 670 nm almost immediately upon excitation, adding to broad absorption band of the trapped electron from the surface states. Particularly, it is interesting to note that the 670 nm band, which is originated from the porphyrin anion radical as usually observed from many other porphyrins,[45] remains in a nanosecond time scale. Furthermore, a relative yield of the long lifetime component in the time profiles is small compared to the free trititanate nanofibers. These results

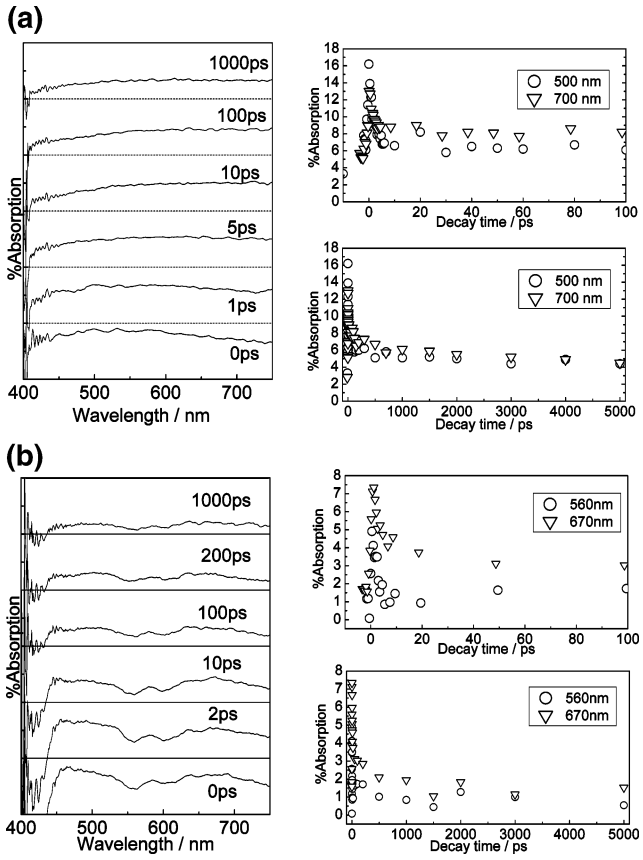

Figure 9. fs-time-resolved transient absorption spectra and decay time profiles of the optically scattering free trititanate nanotubes (a) and SnTTP−TiNFs (b). The time profiles were observed at 500 nm (○) and 700 nm (▽) with decay times 2 ps and 9 ns for trititanate nanotubes and at 560 nm (○) and 670 nm (▽) with decay times 4 ps and 3 ns for SnTTP−TiNFs. Excitation wavelength is 390 nm, and an excitation intensity is about 3 mJ/cm^2.

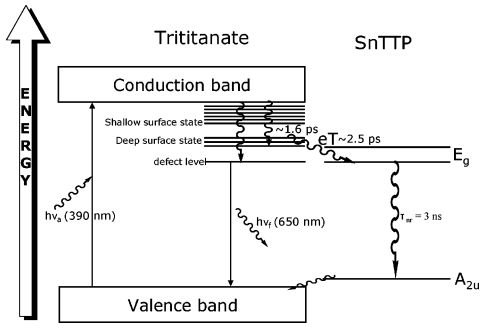

Figure 10. Mechanistic scheme of photoinduced electron-transfer dynamics in SnTTP−TiNFs.

suggest the mechanism of the photoinduced electron transfer as shown in Figure 10. Upon excitation of the trititanate, the exciton is generated and migrated through nonradiative relaxation to deep surface states. Consequently, electrons trapped in the deep surface states are transferred to SnTTP very rapidly in a few picoseconds, forming the SnTTP anion radical of 3 ns lifetime as speculated from the single-nanoparticle fluorescence spectroscopic results. It is interesting to note that the defect sites are not involved in the electron transfer as the single nanoparticle surface emission at 650 nm remains unquenched by SnTTP (Figure 8b).

Photocatalytic Activities. If the photoinduced electrons and holes are well-separated in the SnTTP−TiNFs as discussed above, photooxidation of some organic substrate

(44) Asahi, T.; Furube, A.; Masuhara, H. *Chem. Phys. Lett.* **1997**, *275*, 234−238.
(45) Kim, Y.; Choi, J. R.; Yoon, M.; Furube, A.; Asahi, T.; Masuhara, H. *J. Phys. Chem. B* **2001**, *105*, 8513−8518.

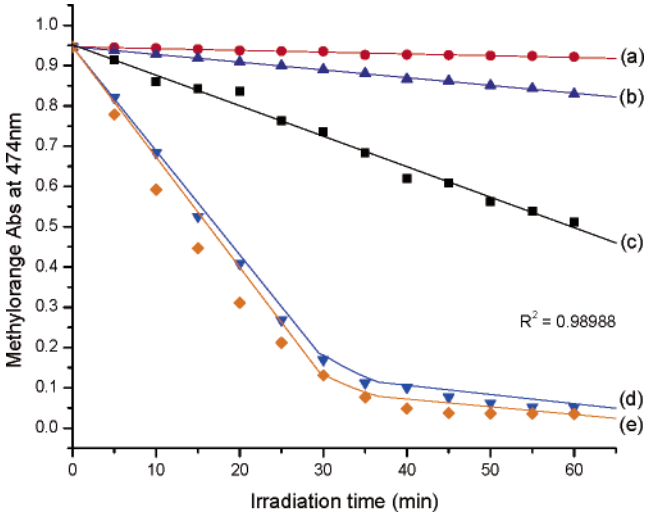

Figure 11. Absorption changes of methyl orange at 474 nm corresponding to photooxidation of methyl orange in aqueous solution containing a mixture of free trititanate nanofibers and SnTPP upon irradiation with visible light (a), free trititanate nanofibers upon irradiation with UV light (b), SnTTP−TiNFs upon irradiation with visible light (c), mixture of free trititanate nanofibers and SnTPP upon irradiation with UV plus visible light (d), SnTTP−TiNFs upon irradiation with UV light (e), and SnTTP−TiNFs upon irradiation with UV plus visible light (f). R^2: correlation coefficient. Intensities of UV and visible lights are 1.08×10^{-8} einstein/min and 6.85×10^{-9} einstein/min, respectively.

would be catalyzed efficiently by the composite SnTTP−TiNFs. Thus, we attempted to assess the photocatalytic oxidation of methyl orange (MO) in aqueous solution (5×10^{-6} M) containing SnTTP−TiNFs, free trititanate nanofibers, and/or SnTTP upon irradiation with UV and/or visible light. Figure 11 shows the plot of relative absorption change of MO at 474 nm as a function of irradiation time under different conditions. The curve (a) shows no absorption change in the presence of free trititanate nanofibers or SnTTP upon visible light irradiation while a slight decrease in absorption was observed in the presence of free trititanate nanofibers upon UV irradiation (curve (b)), indicating that free trititanate nanofibers have very weak UV-sensitive photocatalytic activity without visible light sensitivity. However, it is noteworthy that in the presence of SnTTP−TiNFs the enhanced photooxidation rate was observed (curve (c)) even with visible light irradiation. This may be due to the visible light-sensitive photocatalytic activity of the aggregated SnTTP intercalated into the trititanate layers as reported.[31] Nevertheless, the visible light-sensitive photocatalytic activity of SnTTP−TiNFs is still weaker than the photocatalytic activity (quantum efficiency, 0.15) obtained by irradiation with both UV and visible light as the photooxidation rate was observed to be significantly enhanced even in the aqueous solution MO (curve (d)) containing a simple mixture of free trititanate nanofibers and SnTTP. This implies that the photocatalytic property of SnTTP is synergistically activated by the UV-light-induced generation and consequent transfer of electron from trititanate nanofibers to SnTTP. Supporting this implication, the photooxidation rate of MO in the presence of SnTTP−TiNFs was observed to be tremendously enhanced upon irradiation with UV light only (curve (e)), exhibiting very high photocatalytic quantum efficiency (0.33). This must be due to close proximity of the intercalated SnTTP with trititanate layer as compared to the simple mixture of SnTTP and free trititanate nanofibers. Furthermore, it was found that, upon additional illumination with visible light perpendicular to the UV irradiation, the photocatalytic oxidation of MO was faster with a little higher quantum efficiency (0.35) as compared to the result obtained by illumination with UV light only (curve (f)). This may be due to the visible light-sensitive photocatalytic effect of SnTTP in addition to the photoinduced electron transfer from trititanate layer to SnTTP intercalated. Effects of photoirradiation on stability was examined by observing change of initial rates of the photocatalytic oxidation with the number of the catalyst reuse. As shown in s-Figure 3 (Supporting Information), the SnTTP−TiNFs were observed to be used repetitively for 12 cycles of the photocatalytic reaction with little change of the initial rates under UV−visible light ilumination, indicating high stability of SnTTP intercalated into trititanate nanofibers under the light illumination.

Conclusion

A new class of photoactive composite nanofibers, SnTTP−TiNFs, were synthesized by hydrothermal reaction of a mixture of anatase TiO_2 powders and SnTTP. It was found that the composite nanofibers are spiral multiwalled trititanate ($H_2Ti_3O_7$)-type nanofibers in which SnTTPs are intercalated so that the porphyrins are linearly aggregated on a coplanar level of the molecular moiety. Based on the photoluminescence and fs-diffuse reflectance transient absorption spectroscopic studies, very efficient photoinduced electron transfer takes place directly from trititanate surface states to SnTTP in the composite nanofibers, inferring that electrons and holes are effectively separated in the SnTTP−TiNFs upon illumination. Subsequently, the SnTTP−TiNFs were observed to have highly efficient photocatalytic activity with high stability under light illumination, which is synergistically enhanced by using both UV and visible light illumination. These results imply that the SnTTP−TiNFs may be very useful for potential application in developing an artificial photosynthetic system mimicking natural plant photosynthetic systems operated by so-called Z-scheme mechanism.[3]

Acknowledgment. This work was supported by Korea Science and Engineering Foundation through the joint research project of the Korea-Japan basic scientific cooperation program (Grant F01-2004-000-10024-0) and special basic science project (Grant R01-2004-000-10446-0).

Supporting Information Available: Single-nanoparticle fluorescence spectral measurements. This material is available free of charge via the Internet at http://pubs.acs.org.

CM0629863